physica status solidi

pss

www.pss-journals.com

reprint

WILEY-VCH

Phys. Status Solidi B **248**, No. 3, 659–666 (2011) / **DOI** 10.1002/pssb.201046246

physica status solidi b
www.pss-b.com
basic solid state physics

Phonon dynamics simulation of TlH_2PO_4 crystal

Yaroslav Shchur*

Institute for Condensed Matter Physics, Svientsitskii Str. 1, 79011 Lviv, Ukraine

Received 12 May 2010, revised 21 June 2010, accepted 23 June 2010
Published online 27 July 2010

Keywords ferroelastics, hydrogen bonds, lattice dynamics, phonons, soft modes, TlH_2PO_4

* Corresponding author: e-mail shchur@ph.icmp.lviv.ua, Phone: +380 322 2707439, Fax: +380 322 2761158

Lattice dynamics of TlH_2PO_4 crystal was simulated within the atomistic semi-empirical approach in high-temperature *Pbcn* and ferroelastic $P2_1/b$ phases. Phonon dispersion relations, partial density of phonon states, dispersion of mean square displacements and isotropic temperature factors were calculated. Using both the lattice dynamics simulation and phenomenological Landau–Ginzburg analysis it was shown that the ferroelastic phase transition occurs due to the bilinear interaction between the soft B_{3g} optical and transverse acoustic $TA_Y(\boldsymbol{k} \,||\, \boldsymbol{b}_3)$ phonon modes. The oxygen–hydrogen interactions within the shorter O_1–$H_1\cdots O_2$ hydrogen bonds play the key role at the ferroelastic phase transition.

1 Introduction TlH_2PO_4 (TDP) is a representative of the well-known class of hydrogen-bonded ferroelectric materials of KH_2PO_4 (KDP) type. Due to the presence in these compounds of the system of hydrogen bonds together with the heavy atoms, the crystals of this type have become model objects in studying ferroic phase transitions.

TDP holds a peculiar place among the other compounds of KDP type. In contrast to the other crystals of this family, TDP and its deuterated analogue TlD_2PO_4 crystallize in the orthorhombic *Pbcn* [1] high-temperature structure. TDP undergoes two structural phase transitions with decreasing temperature at $T_1 = 357$ and $T_N = 230$ K [1–4]. The high-temperature second-order $Pbcn\ (Z=4) \leftrightarrow P2_1/b\ (Z=4)$ phase transition occurs into the ferroelastic phase with $U_{YZ} = U_4$ spontaneous deformation.

The low-temperature $P2_1/b\ (Z=4) \leftrightarrow P\bar{1}\ (Z=16)$ phase transition of a slightly first-order type [2, 4] is accompanied by unit-cell multiplication along *a* and *b* axes.

A peculiar feature of TDP crystal is the presence of two kinds of hydrogen bonds differing in their length. H_1 protons are located on the shorter O_1–$H_1\cdots O_2$ hydrogen bonds connecting the PO_4 groups in zigzag-type chains running along the *c* crystallographic axis. Longer O_3–$H_2\cdots O_4$ hydrogen bonds containing the H_2 protons link the *c*-axis running chains of PO_4 groups into an (*a*, *c*) network of PO_4 groups and hydrogen bonds [1–5].

It is accepted [1–4] that both types of protons may, with equal probability, occupy the two possible positions on hydrogen bonds. The ferroelastic $Pbcn \leftrightarrow P2_1/b$ phase transition is accompanied by the ordering of the H_2 hydrogen atoms, whereas H_1 protons are still disordered on hydrogen bonds. However, H_1 protons become ordered below the low-temperature transition into triclinic phase.

TDP was intensively studied by means of various experimental methods. Careful structural research was carried out by different investigators in all temperature phases [1–5]. An exhaustive set of Brillouin scattering [6], elastic [7], resonance [8–12], dielectric [13–16] and spectroscopic [17, 18] measurements have been performed over the last three decades. However, despite the extensive bibliography devoted to the investigation of TDP crystal, one cannot claim that all the aspects of physical properties of this crystal are properly understood. This especially concerns the mechanism of the ferroelastic phase transition, which is not clear so far. According to Brillouin scattering experiments [6], the shear U_{YZ} spontaneous deformation appears due to the softening of the transverse acoustic TA_{YZ} (C_{44}) mode. Ultrasonic measurements revealed a large anomaly of the C_{44} elastic constant in the vicinity of the phase-transition T_1 point [7]. Hanazawa et al. [7] suggested that the acoustic phonon softening is caused by the bilinear coupling with the *Q* transition parameter transforming in the Brillouin zone

(BZ) centre according to the B_{3g} representation of the *Pbcn* space group. Since an X-ray study showed that a slight rotation of PO_4 groups appeared after phase transition into ferroelastic phase [5], Hanazawa et al. [7] suggested that the Q transition parameter may be related to the rotational mode of PO_4 groups. However, a temperature-dependent Raman study revealed no visible softening of the optical mode in the vicinity of the ferroelastic phase transition [18]. Moreover, based on the examination of the isotope effect in the partly deuterated $Tl(H_{1-x}D_x)_2PO_4$ compound, Matsuo et al. [5] arrived at a conclusion that the hydrogen bonds play no significant role in the ferroelastic phase transition. This is a rather unexpected statement, since the protons deposited on longer O_3–H_2···O_4 hydrogen bonds become ordered at this phase transition.

Therefore, there still remain a few questions that need to be answered. Firstly, whether the ferroelastic state appears only due to the acoustic mode instability or whether it is caused by the bilinear interaction between the acoustic and soft optical modes? Secondly, do the protons really play any significant role at this phase transition?

The current research is mainly focused on the study of lattice dynamics peculiarities occurring in two crystal phases, namely the high-temperature *Pbcn* and ferroelastic $P2_1/b$ phases. Special efforts were made for elucidating the ferroelastic phase transition. Apparently, the present study will help to clarify a rather intriguing scenario of this phase transition.

2 Model A lattice dynamics simulation was carried out within the quasi-harmonic approach in two structural *Pbcn* and $P2_1/b$ phases using the following interatomic potential function:

$$\Phi(\rho_{kk'}) = \frac{e^2}{4\pi\varepsilon_0}\frac{Z(k)Z(k')}{r_{kk'}} + a\,\exp\left(-\frac{b\,r_{kk'}}{R(k)+R(k')}\right) + D_j\,\exp\left(-\frac{n_j}{2}\frac{(r_{kk'}-r_{0j})^2}{r_{kk'}}\right), \quad (1)$$

where the first term corresponds to Coulomb, the second to short-range Born–Mayer type and the third to covalent interactions. The third term in Eq. (1) was also used for the simulation of oxygen–hydrogen interactions within the hydrogen bonds. $Z(k)$ and $R(k)$ are the effective charge and radius, respectively, of the kth kind of atom, $a = 1822$ eV and $b = 12.364$ are constants and $r_{kk'}$ is the distance between the atoms of k and k' types. D_j, n_j and r_{0j} are treated as model parameters. However, the values of all parameters utilized for simulating the oxygen–phosphorus interactions within the PO_4 groups (r_{01}, D_{01}, n_1) and oxygen–hydrogen interactions within the hydrogen bonds (D_{02}, n_2) were kept the same in the present work as those already used for other hydrogen-bonded crystals of KDP type [19]. In that sense, the atomistic potential appears to be transferable for different crystals of the KDP family.

Since the r_{0j} parameters related to the length of hydrogen bonds are dependent on a certain crystal structure, we choose them as follows: $r_{02} = 1.397$ Å for shorter O_1–H_1···O_2 and $r_{03} = 1.403$ Å for longer O_3–H_2···O_4 hydrogen bonds in the high-temperature *Pbcn* phase. To preserve the mirror symmetry, we supposed the H atoms to be deposited at the middle of hydrogen bonds. The experimental data concerning the crystal structure determined in two structural phases [1, 4] were used in our simulation. Note that all values of model parameters were adjusted based on the lattice stability conditions. Finally, we obtained the following values of model parameters in *Pbcn* phase: $Z(\mathrm{Tl}) = 0.97$, $Z(\mathrm{P}) = 1.93$, $Z(\mathrm{O}) = -1.0$, $Z(\mathrm{H}) = 0.55$, $R(\mathrm{Tl}) = 2.581$ Å, $R(\mathrm{O}_1) = R(\mathrm{O}_2) = 1.399$ Å, $R(\mathrm{O}_3) = R(\mathrm{O}_4) = 1.424$ Å.

Due to the ordering of H_2 protons in one of two possible positions in hydrogen bonds occurring in the ferroelastic $P2_1/b$ phase and the subsequent electron density redistribution within the O_3–H_2···O_4 hydrogen bonds, some effective charges and radii were slightly changed, namely $Z(\mathrm{Tl}) = 0.99$, $Z(\mathrm{O}_3) = Z(\mathrm{O}_4) = -1.01$, $R(\mathrm{O}_3) = 1.408$ Å and $R(\mathrm{O}_4) = 1.392$ Å. Moreover, two different model parameters $r_{03} = 1.411$ Å and $r_{04} = 1.383$ Å were employed for adequate description of the off-centre location of H_2 protons in ferroelastic phase in $P2_1/b$ phase instead of one r_{02} parameter in *Pbcn* phase.

3 Results and discussion

3.1 Phonons near BZ centre Ninety-six phonon modes of TDP are classified in high-temperature *Pbcn* phase according to irreducible representations in the Γ point as follows: $9A_g + 12B_{1g} + 9B_{2g} + 12B_{3g} + 12A_u + 15B_{1u} + 12B_{2u} + 15B_{3u}$. All the gerade A_g, B_{1g}, B_{2g} and B_{3g} phonon modes are active in Raman spectra, whereas the ungerade modes are active in IR spectra. A_u modes are neither Raman nor IR active. Since the ferroelastic phase transition into $P2_1/b$ phase is associated with the centre of the BZ, the total number of normal modes remains unchanged below T_l. Therefore, 96 phonons have the following symmetry systematization in $P2_1/b$ phase (Γ point): $21A_g + 21B_g + 27A_u + 27B_u$. Similarly to the *Pbcn* phase, all gerade A_g and B_g modes are Raman active, while the ungerade A_u and B_u modes are IR-active modes.

A comparison between the calculated near the BZ centre and experimental phonon frequencies taken in Raman and IR [18] measurements in prototype phase is presented in Table 1. The mode assignment performed basing on the eigenvector analysis is also presented there. It is worth noting that all the experimental frequencies listed in this table were taken in unpolarized spectra. Therefore, their symmetry assignment suggested in Ref. [18] is of a rather approximate character. Moreover, it should be taken into account that the current simulation was done assuming a few requirements imposed by symmetry. First of all, we assumed the regular mirror plane symmetry of PO_4 groups, as follows from *Pbcn* symmetry of prototype phase. Then, to preserve the centric symmetry of high-temperature phase we assumed the hydrogen atoms to be placed in the middle of hydrogen

Table 1 Comparison between the calculated (BZ centre) and experimental [18] optical phonon frequencies (in cm^{-1}) of TDP in high-temperature *Pbcn* phase. H corresponds to the proton modes; $\nu_1 = 940$, $\nu_2 = 420$, $\nu_3 = 1020$ and $\nu_4 = 560\,cm^{-1}$ are the internal modes of PO_4 tetrahedra [20].

A_g		B_{1g}		B_{2g}		B_{3g}		A_u
calc.	exp.	calc.	exp.	calc.	exp.	calc.	exp.	exp.
54	45	30	26	52		23	17	43
137		39	34	144		31	27	115
257	228	43	45	264	358	45		142
ν_2 348		122	92	ν_2 371	475	130	546	251
ν_2 492	546	173		ν_2 496	545	307		ν_2 349
ν_4 534	925	305	1085	ν_4 547	925	ν_2 370	1085	ν_4 502
H_2 916		ν_2 372	1107	H_2 952		ν_2 545		H_1 698
ν_1 1000	1085	ν_2 546	2700	ν_1 1016	1107	H_2 907	2700	H_1 821
ν_3 1166		H_2 856		ν_3 1188		ν_3 1096		$H_2 + \nu_1$ 933
		ν_3 1087				ν_3 1180		$H_2 + \nu_1$ 985
		ν_3 1176				H_2 2803		ν_3 1167
		H_2 2804						H_1 2923

B_{1u}			B_{2u}			B_{3u}		
calc.		exp.	calc.		exp.	calc.		exp.
TO	LO		TO	LO		TO	LO	
24	25		117	134		13	15	
55	55		142	144		52	79	
85	115		245	253		96	102	
150	154		ν_2 356	376	380	154	155	
176	177		ν_4 516	516	530	171	177	
321	332		H_1 672	699		ν_2 319	320	
ν_2 347	349	380	H_1 838	846	860	ν_2 351	376	380
H_1 590	642		H_2 895	950		H_1 589	591	
H_1 732	737	860	ν_1 983	997		H_1 733	804	860
H_2 848	924	1080	ν_3 1124	1190		H_2 897	904	1080
ν_3 1086	1101		H_1 2907	2923	2840	ν_3 1097	1124	
$H_2 + \nu_3$ 1141	1199	2680				ν_3 1143	1172	2840
H_2 2804	2808	2840				H_2 2803	2826	
H_1 2882	2889					H_1 2882	2891	

bonds. This is a rather controversial assumption from many points of view. The split position of hydrogen atoms located in hydrogen bonds was recognized in neutron scattering experiments in TDP at rather low temperatures [4]. It is usually accepted that the same situation is relevant for protons at higher temperatures in prototype phase. However, according to spectroscopic measurements in many hydrogen-bonded crystals of KDP type, namely CsH_2PO_4, CsD_2PO_4 [21], RbD_2PO_4 [22, 23], TlH_2PO_4 [18], TlH_2AsO_4 [24] and $PbHPO_4$ [25, 26], the selection rules are often violated within the region of internal modes of PO_4 groups. This means that on the time scale of internal vibrations ($\sim 10^{-13}$ s) the site symmetry of H_2PO_4 complexes is lower than the symmetry correlated with the factor group symmetry of the high-temperature phase. In other words, on the time scale of internal vibrations, the PO_4 groups should not have a regular shape inherent to the *Pbcn* space group, and the protons should be localized in one of two possible positions on hydrogen bonds. Obviously, the flip-flop motion of protons on hydrogen bonds is correlated with the reorientation motion of PO_4 groups. This complicated phenomenon could not be immediately taken into account in our lattice dynamics simulation. Therefore, we operated with the averaged C_{2v} site symmetry of H_2PO_4 groups in prototype phase, placing the protons in the middle of hydrogen bonds. The difference between the instantaneous and averaged site symmetries evokes a disagreement between the calculated and experimentally observed phonon frequencies presented in Table 1. Therefore, all the calculated phonon frequencies should be treated as the modes intrinsic to a regular orthorhombic structure. The overall discrepancy between the experiment and our simulation amounts to 8.6, 10.0, 5.8, 8.2, 3.5, 3.6 and 3.8% for frequencies of A_g, B_{1g}, B_{2g}, B_{3g}, B_{1u}, B_{2u} and B_{3u} phonon modes, respectively.

A comparison between the experimental [17, 18] and calculated near the BZ centre in ferroelastic $P2_1/b$ phase phonon frequencies is presented in Table 2. The values of TO

Table 2 Comparison between the calculated (BZ centre) and experimental [17, 18] optical phonon frequencies (in cm^{-1}) of TDP in ferroelastic $P2_1/b$ phase. The angles φ correspond to the direction of LO phonon modes counting clockwise from the crystallographic c-axis ($X \perp (b, c)$, $Y \parallel b$, $Z \parallel c$; X, Y and Z are axes of Cartesian system).

A_g		B_g		A_u			B_u			
calc.	exp. [17, 18]	calc.	exp. [17, 18]	calc.		exp. (TO) [18]	calc.			exp. [18]
				TO	LO		TO	LO	φ (°)	
30	28	36	27	16	17		28	29	–70	
38	36	41	44	52	53	52	72	75	40	62
59	46	63	60	71	98		105	114	2	80
82	85	81	97	111	112	90	131	133	83	130
140	105	135	132	114	114	150	194	196	47	195
161		167	175	194	196		213	214	66	
230	237	225	242	216	217	207	236	236	88	
278		280	272	234	235		287	292	40	
320	362	338		281	281		ν_2 347	357	36	
ν_2 360		ν_2 370	365	ν_2 349	349	350	ν_2 357	361	60	
ν_2 408	483	ν_2 416		ν_2 351	366		ν_2 389	407	52	390
ν_2 499	546	ν_2 505	487	ν_2 387	397		ν_2 523	524	25	530
ν_2 546	568	ν_2 557	544	ν_2 509	509	530	$H_1 + \nu_4$ 619	663	5	
ν_4 583		ν_4 585		$H_1 + \nu_4$ 616	617		H_1 688	704	58	
H_3 886		H_3 841		H_1 702	724		H_2 776	793	64	
$H_3 + \nu_1$ 927		$H_3 + \nu_1$ 944	920	H_2 788	822		H_3 834	856	24	
$H_3 + \nu_1$ 963	1085	$H_3 + \nu_1$ 995	1107	H_3 835	839		H_2 861	903	18	
ν_3 1073		ν_3 1067		H_2 890	896		$H_3 + \nu_1$ 912	939	63	
ν_3 1140	2700	ν_3 1136		$H_3 + \nu_1$ 927	928		$H_3 + \nu_1$ 964	990	79	960
ν_3 1160		ν_3 1182		$H_3 + \nu_1$ 971	975	960	ν_3 1061	1072	54	1065
H_3 2768		H_3 2768		ν_3 1071	1107	1065	ν_3 1099	1124	15	
				ν_3 1109	1122		ν_3 1176	1187	73	
				ν_3 1163	1177		H_3 2768	2772	9	2670
				H_3 2767	2790		H_2 2864	2871	17	
				H_2 2865	2873		H_1 2899	2915	87	
				H_1 2915	2915					

and LO mode frequencies of B_u type were obtained through the angle scanning of the phonon spectrum in the monoclinic (b, c) plane around the Γ point. Note that all the experimental B_u frequencies are of a mixed TO–LO type. Disagreement between the theory and experiment is 7.6, 7.0, 7.2 and 5.9% for A_g, B_g, A_u and B_u irreducible representations, respectively. However, we should bear in mind that the experimental frequencies of dipole-active B_u modes were obtained using an inadequate experimental technique. It is known [27] that a special three-polarization IR experimental set-up is needed to properly determine the parameters of phonon modes vibrating within the monoclinic (b, c) plane. Despite the fact that the angle of monoclinicity is rather small ($\alpha = 91.67^\circ$ [4]) in ferroelastic phase, the directions of the dipole moment of phonon modes (direction of longitudinal modes) do not coincide with Cartesian Y and Z axes but constitute certain angles with these axes. The angles φ calculated within the present simulation are listed in Table 2. The inadequacy of the experimental method used in determining the B_u modes may be another reason for disagreement between the calculated and measured frequencies presented in Table 2.

3.2 Phonon spectrum and mechanism of ferroelastic phase transition The investigation of phonon dispersion relations enables us to discover some intrinsic peculiarities of the transition mechanism. Figure 1 demonstrates the low-frequency part of the phonon spectrum calculated along the $\boldsymbol{b}_2$ direction of the BZ. Only dispersion curves transforming according to the Δ_4 irreducible representation of the $\boldsymbol{k} = \mu \boldsymbol{b}_2$ $(0 < \mu < 1/2)$ wave vector group are presented there. We restricted our consideration to the lowest energy range of the spectrum since the phonon dynamics in this region eventually plays the most significant role at phase transitions. Dashed lines labelled by the number '1' correspond to the spectrum calculated using the lattice parameters obtained at $T = 373$ K [1] and relaxed to satisfy the lattice stability conditions ($a = 4.534$ Å, $b = 14.380$ Å, $c = 6.540$ Å). The lowest phonon mode is an acoustic branch of B_{1u} symmetry and the two lowest frequency optical branches have the B_{3g} and B_{1u} symmetries, respectively (hereafter the symmetry indication corresponds to the Γ point). Dotted dispersion lines labelled in Fig. 1 by the number '2' were simulated using the lattice parameters corrected by the linear thermal expansion [7]. We used the

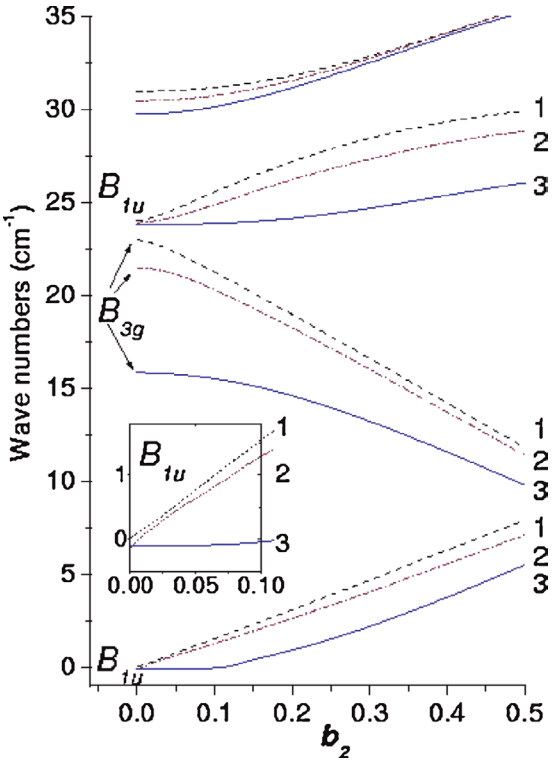

Figure 1 (online colour at: www.pss-b.com) Low-frequency part of phonon spectrum calculated along b_2 axis of BZ in *Pbcn* phase. The meaning of the numbers 1, 2 and 3 is explained in the text. The dispersion of the B_{1u} acoustic mode close to the Γ point is presented in the inset.

following values $a_{357\,K} = 4.531$ Å, $b_{357\,K} = 14.363$ Å, $c_{357\,K} = 6.535$ Å close to the phase-transition point $T = 357$ K. Utilization of the new values of the lattice parameters should imply the overall effects of lattice anharmonicity being indirectly and qualitatively taken into account. All model parameters were kept unchanged. Phosphorus–oxygen distances within the PO_4 groups were retained constant since these covalent-bonded distances are almost temperature independent within the *Pbcn* phase. As seen in Fig. 1, there is a slowing down of all the optical dispersion curves and a decrease of the tilt of the B_{1u} acoustic branch calculated at $T = 357$ K. According to the eigenvector analysis, the transverse acoustic B_{1u} mode is polarized along the Z direction ($X \,||\, a$, $Y \,||\, b$, $Z \,||\, a$ in *Pbcn* phase). Since this mode propagates along the $\boldsymbol{b}_2$ axis (Y direction), the eventual slowing down of the slope of this acoustic branch should evoke the appearance of macroscopic $U_{YZ} = U_4$ spontaneous deformation. So, even with the indirect accounting of the anharmonic interphonon effects through the lattice thermal expansion, the quasi-harmonic lattice dynamics simulation considers the principal physical mechanism leading to the ferroelastic phase transition.

In order to mimic the conditions that might lead to zero slope of the B_{1u} acoustic branch, i.e. to the ferroelastic phase transition, we investigated the conditions of the loss of lattice stability. We based this on a simple physical assumption. Since the second-order ferroelastic $Pbcn \leftrightarrow P2_1/b$ phase transition is accompanied by redistribution of H_2 protons on the hydrogen bonds, we assumed that oxygen–hydrogen interactions gradually change within the hydrogen bonds even in the high-temperature *Pbcn* phase. We have found that the slight variation (order of 0.01–1%) of model parameters corresponding to interatomic interactions within the hydrogen bonds evokes drastic changes in phonon dynamics. It was suggested earlier in Ref. [28] that the order–disorder character of pretransitional fluctuations governs the phase transition in TlD_2PO_4. A similar situation should be expected in TDP. According to our simulation, the most crucial impact on the low-frequency phonon dynamics is made by the H_1 protons, which still remain disordered on the shorter hydrogen bonds in ferroelastic phase. As seen in Fig. 1 (solid lines labelled by the number '3'), the 0.35% change of the r_{02} parameter corresponding to the O_1–H_1 and O_1–H_2 interactions from 1.397 to 1.4019 Å evokes the falling of the slope of the B_{1u} acoustic branch down to zero close to the BZ centre. The freezing of the B_{1u} acoustic mode implies the appearance of the ferroelastic phase with the uniform U_4 spontaneous deformation. This critical behaviour of the acoustic mode is accompanied by a significant decrease (nearly 26%) of the lowest B_{3g} optical mode close to the Γ point. All other optical modes change rather little with the exception of only the B_{3g} mode (near 43 cm^{-1}), which diminishes by nearly 11%.

According to group theory analysis, the symmetry $Pbcn \leftrightarrow P2_1/b$ transformation occurring in the Γ point should be realized owing to the activity of the B_{3g} irreducible representation. A clear correlation between the softening of the B_{3g} optical mode and the falling down of the B_{1u} acoustic branch may be easily explained within the phenomenological Landau–Ginzburg theory. The quasi-harmonic contribution to the free-energy density function may be written as follows [7, 29]:

$$f = \frac{1}{2}A_0(T - T_1)Q^2 + \frac{1}{2}\gamma\left(\frac{\partial Q}{\partial Y}\right)^2 + \alpha Q U_4 + \frac{1}{2}C_{44}^0 U_4^2, \tag{2}$$

where Q is the normal coordinate of the soft phonon mode and C_{44}^0 is the elastic constant far from the phase-transition point. Since the $Pbcn \leftrightarrow P2_1/b$ phase transition is governed by the B_{3g} irreducible representation, Q is treated here to be transformed according to the B_{3g} representation as well. Replacing U_4 in Eq. (2) by $U_{YZ} = \partial Z/\partial Y$ (the eigenvector of the B_{1u} acoustic mode has only a Z component) and using the Fourier transform, one may rewrite the free-energy function as follows:

$$F = \int f \mathrm{d}y = \sum_k \frac{1}{2}\omega_0^2(\boldsymbol{k})Q_k Q_k^* + \frac{1}{2}\omega_{TA}^2(\boldsymbol{k})Z_k Z_k^* + i\alpha\boldsymbol{k}(Z_k Q_k^* - Q_k Z_k^*). \tag{3}$$

The Q_k and Z_k normal coordinates correspond to the soft optical B_{3g} and the transverse acoustic B_{1u} mode, respectively. 'Uncoupled' frequencies of these modes may be presented in the close vicinity to the Γ point as

$$\omega_0^2(\boldsymbol{k}) = A_0(T - T_l) + \gamma \boldsymbol{k}^2 + \ldots,$$
$$\omega_{\mathrm{TA}}^2(\boldsymbol{k}) = C_{44}^0 \boldsymbol{k}^2 + \ldots \tag{4}$$

Constructing the Lagrangian

$$L = T - F = \frac{1}{2}\sum_k \left(\dot{Q}_k \dot{Q}_k^* + \dot{Z}_k \dot{Z}_k^*\right) - F, \tag{5}$$

and solving the Lagrange equation of motion similarly to Ref. [29], one may obtain the frequencies of 'coupled' phonon modes:

$$\Omega_{\pm}^2 = \frac{1}{2}\left(\omega_0^2 + \omega_{\mathrm{TA}}^2 \pm \sqrt{\left(\omega_0^2 - \omega_{\mathrm{TA}}^2\right)^2 + 4\alpha^2 \boldsymbol{k}^2}\right). \tag{6}$$

The bilinear interaction between the soft optical and acoustic modes evokes the 'repulsion' of these modes and consequently the decrease of the slope of the 'coupled' Ω_- mode. The phase transition into ferroelastic phase occurs when the slope $\mathrm{d}\Omega_-/\mathrm{d}\boldsymbol{k}$ of this Ω_- branch equals zero or, in other words, when

$$\omega_0^2 \omega_{\mathrm{TA}}^2 = \alpha^2 \boldsymbol{k}^2. \tag{7}$$

It follows from Eq. (7) that in the $\boldsymbol{k} \to 0$ limit the ferroelastic phase transition may occur at the temperature

$$T_l = T_C + \frac{\alpha^2}{A_0 C_{44}^0}, \tag{8}$$

where the soft mode ω_0 frequency still remains positive, whereas the tilt of the acoustic branch demonstrates the critical slowing down.

As seen, the phenomenological theory describes the physical mechanism of the process simulated by us within the lattice dynamics approach and presented in Fig. 1. According to the current simulation, the H_1 protons play the crucial role in softening the lowest B_{3g} optical mode and in falling down of the B_{1u} acoustic branch. The significance of the influence exerted by the H_1 hydrogen atoms upon the ferroelastic phase transition may be clarified by means of the analysis of the partial density of phonon states (PDOS) function calculated in *Pbcn* phase (see Fig. 2). This function is related to the frequency dispersion of eigenvectors of a certain type of atom. Figure 2 presents the low-frequency region (0–275 cm^{-1}) of the PDOS of the atoms involved in shorter O_1–$H_1\cdots O_2$ and longer O_3–$H_2\cdots O_4$ hydrogen bonds in high-temperature *Pbcn* phase. As seen in this figure, there is a quite definite contribution of H_1 atoms into external lattice vibrations within the 75–260 cm^{-1} region, whereas the contribution of H_2 atoms appears to be almost negligible there. Moreover, the contribution of O_1 and O_2 oxygen atoms involved in O_1–$H_1\cdots O_2$ hydrogen bonds into these mixed

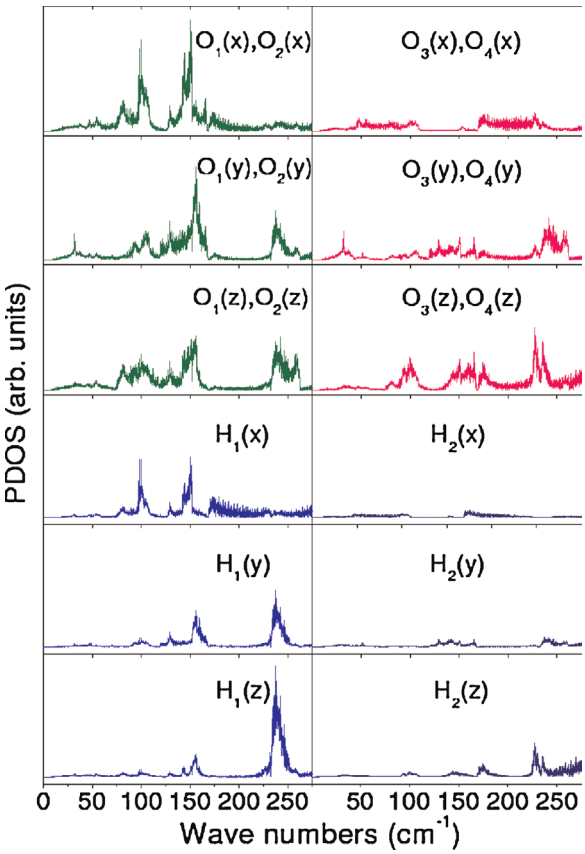

Figure 2 (online colour at: www.pss-b.com) Low-frequency part of PDOS spectra simulated in *Pbcn* phase. Only the atoms involved in O_1–$H_1\cdots O_2$ and O_3–$H_2\cdots O_4$ hydrogen bonds are presented here.

low-frequency lattice vibrations is much stronger compared with the contribution of O_3 and O_4 atoms.

The frequency dispersion of mean square displacements of oxygen and hydrogen atoms simulated in *Pbcn* phase (see Fig. 3) is also rather indicative. As seen from this figure, the H_1 atoms vibrate in the 75–165 cm^{-1} region with displacements several times larger than the H_2 protons. The similar correlation between the values of atomic displacements in this frequency range is also relevant for O_1 (O_2) and O_3 (O_4) atoms. Generally, both the experiment and our simulation give a larger value for the isotropic temperature factors B_{iso} of H_1 protons compared with the values related with the H_2 atoms (see Table 3). Moreover, B_{iso} of H_1 and H_2 protons also shows a clearly visible correlation with the O_1 (O_2) and O_3 (O_4) atoms, respectively. In such conditions, a slight variation in O_1–H_1 or O_2–H_1 interactions may crucially affect the low-frequency phonon dynamics of TDP, leading to the lattice instability.

In order to compare the significance of both types of hydrogen bonds that becomes apparent at the ferroelastic phase transition, it is worth checking the change of the PDOS function occurring in $P2_1/b$ phase. The PDOS of H_1 and H_2 hydrogen atoms in high-temperature *Pbcn* phase is depicted in the right-hand panel of Fig. 4, whereas the PDOS

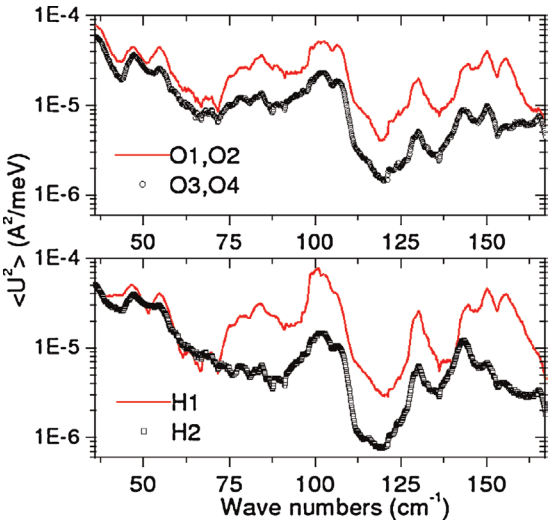

Figure 3 (online colour at: www.pss-b.com) Low-frequency dispersion of mean square displacements of oxygen and hydrogen atoms in *Pbcn* phase. Only the atoms involved in O_1–H_1···O_2 and O_3–H_2···O_4 hydrogen bonds are presented in this figure.

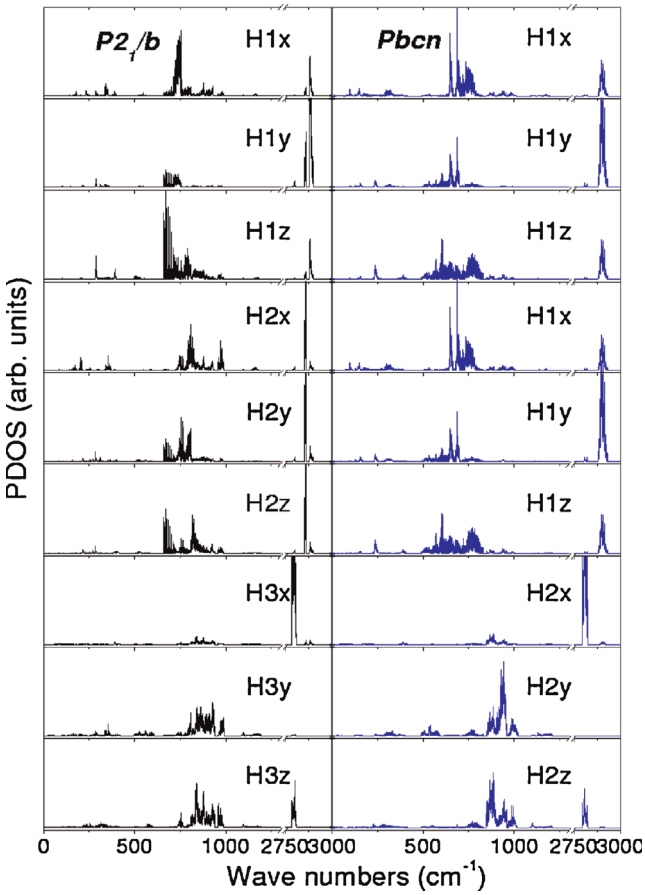

Figure 4 (online colour at: www.pss-b.com) PDOS spectra of hydrogen atoms calculated in *Pbcn* and $P2_1/b$ phases.

corresponding to H_1, H_2 and H_3 protons in $P2_1/b$ phase is presented in the left-hand panel of Fig. 4. Note that the H_1 atoms being still disordered in ferroelastic phase become there structurally separated into two H_1 and H_2 types [4], whereas the hydrogen atoms ordered on the longer hydrogen bonds at room temperature change their labelling from H_2 in *Pbcn* phase to H_3 in $P2_1/b$ phase. In order to simplify the comparison between the data of both temperature phases, the PDOS of H_1 atoms is presented twice in *Pbcn* phase. As seen in this figure, the *X*, *Y* and *Z* components of the PDOS of H_2 atoms in *Pbcn* phase remain almost invariable in ferroelastic phase (H_3 atoms in $P2_1/b$ phase). There is only a shift down in $P2_1/b$ phase of the order of 40 cm^{-1} of H_3 modes polarized in the (*Y*, *Z*) plane in the region corresponding to stretching vibrations of PO_4 groups. Such a small change is a rather unexpected result since the H_2 protons disordered above the phase transition T_1 point (within the current simulation they were treated to be placed in the middle of hydrogen bonds) become ordered in one of the two off-centre positions in $P2_1/b$ phase. However, even the ordering of H_2 protons in hydrogen bonds occurring in ferroelastic phase does not significantly affect the PDOS function. Rios et al. [2] prejudiced against the possibility for H_2 protons to be disordered in the double-well potential in high-temperature phase. If this statement is true, it should explain the moderate changes of the PDOS spectra of H_2 atoms at the ferroelastic phase transition.

A different situation is observed for H_1 protons (H_1 labelling corresponds to *Pbcn*), which still remain disordered in ferroelastic phase (labelled there as H_1 and H_2). First of all, there is a distinct difference in $P2_1/b$ phase between the PDOS of H_1 and H_2 atoms located on the shorter hydrogen bonds. The same difference is observed for B_{iso} of H_1 and H_2 protons (see Table 3). The vibrations of H_1 atoms are mainly polarized in the (*X*, *Z*) plane within the region corresponding to both the bending and stretching PO_4 vibrations, whereas the vibrations of H_2 protons manifest no visible space anisotropy. There is a shift near 150 cm^{-1} to higher frequencies of H_2 modes located in the region of bending vibrations of PO_4 groups in $P2_1/b$ phase. All these changes in vibration spectra of H_1 and H_2 protons in $P2_1/b$ phase are

Table 3 Comparison between the calculated and experimental [1, 4] isotropic temperature factors B_{iso} of TDP in high-temperature *Pbcn* and ferroelastic $P2_1/b$ phases.

Pbcn			$P2_1/b$		
type of ions	calc.	exp. [1]	type of ions	calc.	exp. [4]
Tl	3.47	4.02	Tl	2.54	3.06
P	3.27	2.52	P	2.37	1.89
O_1, O_2	4.38	5.68	O_1	2.67	4.15
O_3, O_4	3.45	3.79	O_2	2.66	3.29
H_1	5.79	5.76	O_3	2.45	2.78
H_2	4.48	4.97	O_4	2.51	2.68
			H_1	3.78	3.31
			H_2	3.90	4.20
			H_3	3.65	4.07

correlated with the corresponding changes of O_1 and O_2 oxygen atoms involved in the shorter O_1–$H_1(H_2)\cdots O_2$ hydrogen bonds. A smaller shift up near 50 cm^{-1} is observed for these hydrogen modes in the region of external lattice vibrations (100–320 cm^{-1}). Isotropic temperature factors B_{iso} of O_1 and O_2 atoms involved in the shorter hydrogen bonds with the disordered H_1 and H_2 protons are larger in $P2_1/b$ phase than B_{iso} of O_3 and O_4 atoms (see Table 3). Therefore, one may infer that the PDOS spectra and the B_{iso} data of atoms deposited on the shorter O_1–$H_1(H_2)\cdots O_2$ hydrogen bonds manifest distinct changes in two structural phases (*Pbcn* and $P2_1/b$). Obviously, the dynamics of H_1 protons plays the relevant role in the mechanism of *Pbcn* and $P2_1/b$ phase transitions.

4 Summary A lattice dynamics study of TDP crystal was carried out within the semi-phenomenological atomistic approach in two structural phases. We have found that the same empirical model parameters related to the covalent-bonded interaction within the PO_4 groups and within the hydrogen O–H···O bonds quite reasonably describe the lattice dynamics of different hydrogen-bonded crystals of KDP type.

Based on analysis of the calculated phonon spectra, PDOS and isotropic temperature factor of constituent atoms, it was established that the oxygen–hydrogen interactions within the shorter O_1–$H_1\cdots O_2$ hydrogen bonds play the key role in the ferroelastic phase transition. The $Pbcn \leftrightarrow P2_1/b$ phase transition occurs due to the bilinear interaction between the soft B_{3g} optical and acoustic B_{1u} modes, as was earlier suggested in Ref. [7]. The softening of the lowest frequency B_{3g} optical mode is accompanied by the falling down of the B_{1u} acoustic branch close to the BZ centre. The point of the ferroelastic phase transition corresponds to the zero slope of the acoustic branch and the appearance of uniform U_{YZ} spontaneous deformation. The soft B_{3g} optical mode remains positive in the phase-transition point. Since no visible softening has been observed in the former Raman investigations close to the ferroelastic phase transition of TDP, new precise spectroscopic experiments would be of high interest.

Acknowledgements The author would like to thank Prof. I. V. Stasyuk for fruitful discussion of the obtained results.

References

[1] S. Rios, W. Paulus, A. Cousson, M. Quilichini, G. Heger, N. Le Calve, and B. Pasquier, J. Phys. I France **5**, 763 (1995).
[2] S. Rios, W. Paulus, A. Cousson, M. Quilichini, and G. Heger, Acta Crystallogr. B **54**, 790 (1998).
[3] E. Alvarez-Otero, G. Madariga, I. Peral, C. L. Folcia, and S. Rios, Acta Crystallogr. B **58**, 750 (2002).
[4] I. H. Oh, M. Merz, S. Mattauch, and G. Heger, Acta Crystallogr. B **62**, 719 (2006).
[5] A. Matsuo, K. Irokawa, M. Komukae, T. Osaka, and Y. Makita, J. Phys. Soc. Jpn. **63**, 1626 (1994).
[6] M. Arai, T. Yagi, A. Sakai, M. Komukae, T. Osaka, and Y. Makita, J. Phys. Soc. Jpn. **59**, 1285 (1990).
[7] K. Hanazawa, M. Komukae, T. Osaka, Y. Makita, M. Arai, T. Yagi, and A. Sakai, J. Phys. Soc. Jpn. **60**, 188 (1991).
[8] J. Seliger, V. Zagar, R. Blinc, and V. H. Schmidt, J. Chem. Phys. **88**, 3260 (1988).
[9] S. H. Kim, K. W. Lee, J. W. Jang, C. E. Lee, J. Y. Choi, K.-S. Lee, and J. Kim, Phys. Rev. B **72**, 214107 (2005).
[10] S. H. Kim, K. W. Lee, J. W. Jang, C. E. Lee, K.-S. Lee, and S. J. Noh, Curr. Appl. Phys. **6**, 182 (2006).
[11] S. H. Kim, K. W. Lee, J. H. Han, and C. E. Lee, Solid State Commun. **144**, 1 (2007).
[12] S. H. Kim, K. W. Lee, B. H. Oh, and C. E. Lee, Phys. Rev. B **76**, 172104 (2007).
[13] N. Yasuda, S. Fujimoto, T. Asano, K. Yashino, and Y. Inuishi, J. Phys. D, Appl. Phys. **13**, 83 (1980).
[14] R. Mizeris, J. Grigas, R. N. P. Choudhary, and T. V. Narasaiah, Phys. Status Solidi A **118**, 597 (1989).
[15] J. H. Park, K.-S. Lee, J.-B. Kim, M. Komukae, T. Osaka, and Y. Makita, J. Phys. Soc. Jpn. **66**, 1268 (1997).
[16] K.-S. Lee, S.-H. Kim, C. E. Lee, and I.-H. Oh, J. Phys. Soc. Jpn. **77**, 075002 (2008).
[17] A. De Andres and C. Prieto, Phase Transitions **14**, 3 (1989).
[18] B. Pasquier, N. Le Calve, S. Al Homsi-Teiar, and F. Fillaux, Chem. Phys. **171**, 203 (1993).
[19] Ya. Shchur, Phys. Status Solidi B **244**, 569 (2007); Ya. Shchur, J. Phys.: Condens. Matter **20**, 195212 (2008).
[20] K. Nakamoto, Infrared and Raman Spectra of Inorganic and Coordination Compounds (John Wiley, New York, 1997), p. 387.
[21] B. Marchon and A. Novak, J. Chem. Phys. **78**, 2105 (1983).
[22] B. Marchon, A. Novak, and R. Blinc, J. Raman Spectrosc. **18**, 447 (1987).
[23] Ya. Shchur, V. Dzhala, O. Vlokh, and I. Klymiv, Phys. Status Solidi B **144**, K17 (1994).
[24] K.-S. Lee and D.-H. Ha, Phys. Rev. B **48**, 73 (1993).
[25] D. J. Lockwood and N. Ohno, Ferroelectrics **137**, 181 (1992).
[26] Ya. Shchur, Phys. Status Solidi B **246**, 102 (2009).
[27] A. B. Kuz'menko, E. A. Tishchenko, and V. G. Orlov, J. Phys.: Condens. Matter **8**, 6199 (1996).
[28] S. Rios, M. Quilichini, and J. M. Perez-Mato, J. Phys.: Condens. Matter **10**, 3045 (1998).
[29] A. V. Kityk, Ya. I. Shchur, A. V. Zadorozhna, I. B. Trach, I. S. Girnyk, I. Yu. Martynyuk-Lototska, and O. G. Vlokh, Phys. Rev. B **58**, 2505 (1998).

